Amount of Asian lithospheric mantle subducted during the India/Asia collision

Anne Replumaz *, Stéphane Guillot, Antonio Villaseñor, Ana M. Negredo

Université de Grenoble I, CNRS, BP 53, 38041 Grenoble Cedex, France
Instituto de Ciencias de la Tierra Jaume Almera, CSIC, Sole' i Sabarı's s/n, 08028 Barcelona, Spain
Dept. of Geophysics, Facultad CC. Físicas, Universidad Complutense de Madrid. Av. Complutense, 28040 Madrid, Spain

ARTICLE INFO

ABSTRACT

Body wave seismic tomography is a successful technique for mapping lithospheric material sinking into the mantle. Focusing on the India/Asia collision zone, we postulate the existence of several Asian continental slabs, based on seismic global tomography. We observe a lower mantle positive anomaly between 1100 and 900 km depths, that we interpret as the signature of a past subduction process of Asian lithosphere, based on the anomaly position relative to positive anomalies related to Indian continental slab. We propose that this anomaly provides evidence for south dipping subduction of North Tibet lithospheric mantle, occurring along 3000 km parallel to the Southern Asian margin, and beginning soon after the 45 Ma break-off that detached the Tethys oceanic slab from the Indian continent. We estimate the maximum length of the slab related to the anomaly to be 400 km. Adding 200 km of presently Asian subducting slab beneath Central Tibet, the amount of Asian lithospheric mantle absorbed by continental subduction during the collision is at most 600 km. Using global seismic tomography to resolve the geometry of Asian continent at the onset of collision, we estimate that the convergence absorbed by Asia during the indentation process is ~1300 km. We conclude that Asian continental subduction could accommodate at most 45% of the Asian convergence. The rest of the convergence could have been accommodated by a combination of extrusion and shallow subduction/underthrusting processes. Continental subduction is therefore a major lithospheric process involved in intraplate tectonics of a supercontinent like Eurasia.

© 2012 International Association for Gondwana Research. Published by Elsevier B.V. All rights reserved.

1. Introduction

The long-lasting collision between India and Asia causes profound changes over immense areas, building the Earth's largest and highest topography, and provides unequaled opportunities to study the mechanics of continental deformation (Fig. 1). Global seismic tomography suggests that this extreme topography is related to successive continental subduction episodes of the Indian continent (e.g. Replumaz et al., 2010a). Positive wavespeed anomalies are commonly interpreted as remnants of slabs, and evidences for past Indian subduction episodes are preserved as deep anomalies (IN and TH in blue in Fig. 1). In this paper, we show that global seismic tomography provides also evidence of past Asian continental subduction. We estimate the length of the Asian lithospheric slabs subducted since the beginning of collision, and we calculate the amount of convergence that is absorbed by Asian continental subduction since then.

To do so, we have to know the geometry of the Asian continent at the beginning of collision. Plate tectonic reconstructions constrain the northward motion of the Indian Plate since the mid-Lower Cretaceous (e.g. Patriat and Achache, 1984; Besse and Courtillot, 2002; Molnar and Stock, 2009), but cannot alone resolve the position of the plate boundary between India and Asia at the onset of collision. The southern Asian geometry at that moment has been previously estimated using the present-day geometry of the indentation marks left by the impact of India onto the Asian margin, with a presumably linear geometry between Sumatra and the mouth of the Indus river (e.g. Tapponnier et al., 1986; Le Pichon et al., 1992) or using continental paleomagnetic data (e.g. Halim et al., 1998). Seismic tomography independently constrains the position of the plate boundaries. In particular, the NW–SE-trending positive anomaly beneath India, at depths between 1000 and 1600 km, is thought to record the location of late Mesozoic Tethys subduction (marked as TH in Fig. 1; van der Voo et al., 1999; Replumaz et al., 2004; Hafkenscheid et al., 2006; Richards et al., 2007). The TH anomaly marks the past position of the trench between the Indian and Asian continents (Fig. 1). This anomaly vanishes at depths shallower than about 1100 km, indicating a slab break-off after the beginning of the continental Indian plate subduction, likely when the slab reached a critical length (Chemenda et al., 2000). The paleo-geometry of the Indian continent northern boundary at the time of break-off is drawn along the top of the TH anomaly (Negredo et al., 2007). This boundary is similar to the previously estimated linear geometry between Sumatra and the mouth of the Indus (Tapponnier et al., 1986). By combining the paleo-position of India and the length of the Indian slab as it is now subducting beneath the Hindu Kush, Negredo et al. (2007) inferred the

* Corresponding author.
  E-mail address: anne.replumaz@ujf-grenoble.fr (A. Replumaz).
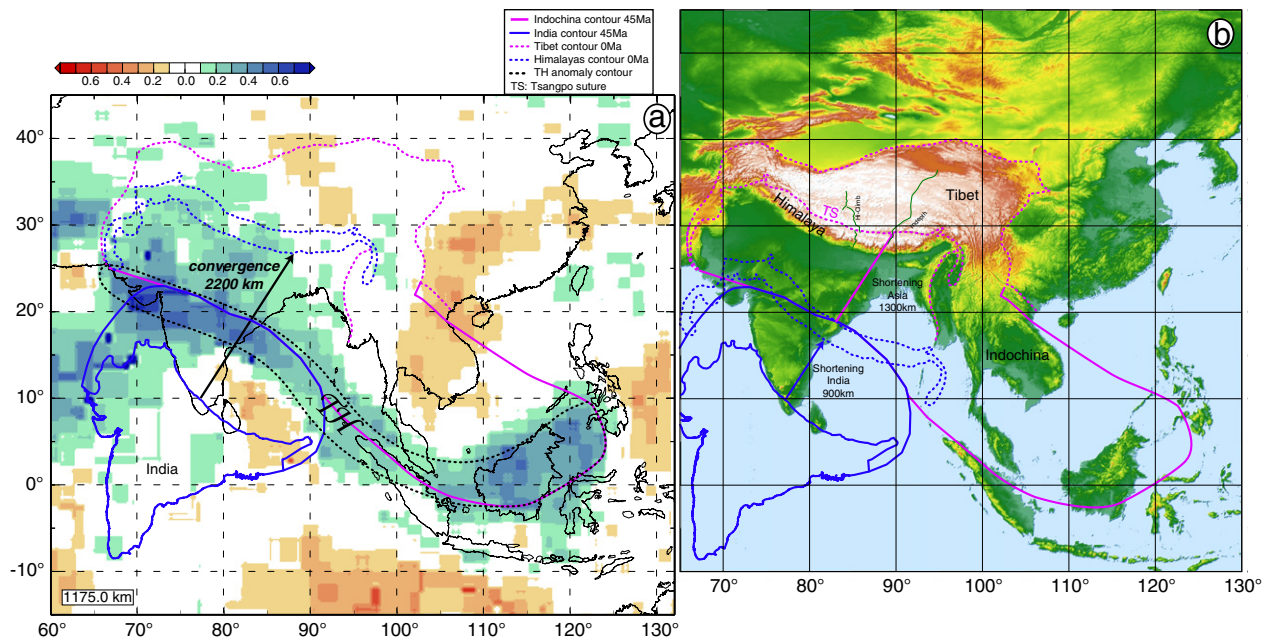
Fig. 1. a) P-wave tomographic section at 1175 km depth showing wavespeed anomaly at −/+ 0.8%, positive anomaly in blue, negative in red. Positive anomaly are related to colder material, commonly interpret as remnant of slab sinking into the mantle. Looking at the anomalies at depth permits to deduced the past position of the subduction zones. Beneath India, the NW–SE-trending anomaly TH is thought to record the location of late Mesozoic Tethys subduction. By using the paleo-position of India and the length of the Indian slab as it is now subducting beneath the Hindu Kush, Negredo et al. (2007) deduced the north–south length of the Indian continent at the indentation initiation and drew the paleo-geometry of the Indian continent northern boundary along the paleo-trench, north of the TH anomaly (blue contour). We measure the distance between the paleo-position of the Himalayan front and its present-day position as an estimation of the convergence, ~2200 km (black arrow). b) Topographic map with approximately the same extend than the tomographic section. We compare the paleo-geometry of Indian continent with the present-day contour of Himalayas (dotted blue line between the Himalayan front and the Tsangpo suture, TS, moved to the position of India at 45 Ma), and Tibet (dotted pink line). We measure the distance between the paleo and the present-day Himalayan front, ~900 km (blue arrow). It is an estimation of the convergence absorbed by India. The distance between the paleo and the present-day Tsangpo suture is ~1300 km (pink arrow). It is an estimation of the convergence absorbed by Asia. (For interpretation of the references to color in this figure legend, the reader is referred to the web version of this article.)

north–south extent of the Indian continent at the time of break-off (blue contour in Fig. 1a) and estimated the age of break-off at ~45 Ma. This age is younger than the 57–55 Ma estimated for the first continent–continent contact, deduced concordantly from exhumation of ultrahigh-pressure rocks (de Sigoyer et al., 2000; Guillot et al., 2003; Leech et al., 2005), the final closure of Neotethys recorded by the end of marine sedimentation at 55 Ma (Garzanti et al., 1987), and the appearance of continental red beds at ~51 Ma (Garzanti et al., 1996). This younger age of break-off suggests that some amount of Indian continental subduction occurred before break-off (e.g. Guillot et al., 2008). This time of slab break-off corresponds to the beginning of the indentation process, when India left behind the detached oceanic slab and began to impinge upon the Asian margin.

Comparing the paleo-geometry of the continents at the time of break-off and the present-day shape of the continents, we estimate the magnitude of convergence absorbed by the post-collisional deformation of the Indian and Asian continents (Fig. 1). The mechanism of deformation of each continent is different. The Indian continent deforms over a narrow area forming the high Himalayan range which grows up by scraping of the upper Indian crust, while the lower crust and underlying lithosphere bend and underthrust the range (Nábělek et al., 2009). Separated from the upper crust, the Indian continental lithosphere is heavy enough to subduct into the mantle (Capitanio et al., 2010). Deep tomographic positive anomalies suggest multiple successive continental subduction episodes of the Indian continent (Replumaz et al., 2010a). The prominent anomaly IN observed between 450 and 900 km depths (Fig. 2) has been interpreted as a slab formed by Indian continental lithosphere which subducted most probably between 40 and 15 Ma beneath central Tibet (Replumaz et al., 2010a). The Asian continental upper plate deforms over a broad area forming the Tibetan Plateau (pink contour Fig. 1b). The Tibetan plateau appears as a homogeneous zone of high elevation that could be generated by a homogeneous deformation process (England and

Houseman, 1988). However very narrow shear zones, ~10 km width but running over several thousands of kilometers and absorbing hundreds of kilometers of displacement (Leloup et al., 2001), suggest that the deformation is localized in the upper crust (Tapponnier et al., 1986; Replumaz and Tapponnier, 2003). In contrast, continental subduction is thought to accommodate convergence at lower crust and lithospheric mantle levels (Mattauer, 1986; Willett and Beaumont, 1994; Tapponnier et al., 2001; De Celles et al., 2002). Seismic profiles show evidence of southward Asian subduction down to 300 km in Central Tibet (e.g. Kind et al., 2002). Toward the western syntax, earthquakes down to 200 km and tomographic positive anomaly down to 400 km reflect on-going southward Asian subduction beneath the Pamir (Burtman and Molnar, 1993; Negredo et al., 2007). The purpose of this paper is to use global deeper seismic tomography to find evidence of older Asian continental slabs and to estimate the amount of the lithospheric mantle of Asia that has been subducted since the beginning of collision.

2. Mantle tomographic positive anomalies beneath the collision zone

2.1. Tomographic model

We investigate the mantle structure beneath the collision zone down to 1500 km depth (Figs. 1 and 2), by means of a P-wave global mantle tomographic model obtain using the method described by Bijwaard et al. (1998), but augmented with additional arrival times from well-located earthquakes at both teleseismic and regional distances (Villaseñor et al., 2003). In total, more than 14 million arrival times from 300,000 earthquakes, nearly 4 times the amount used in Bijwaard et al. (1998), were reprocessed using the EHB methodology (Engdahl et al., 1998). This global model has been already used in several papers focusing on different regions (Replumaz et al., 2010b;
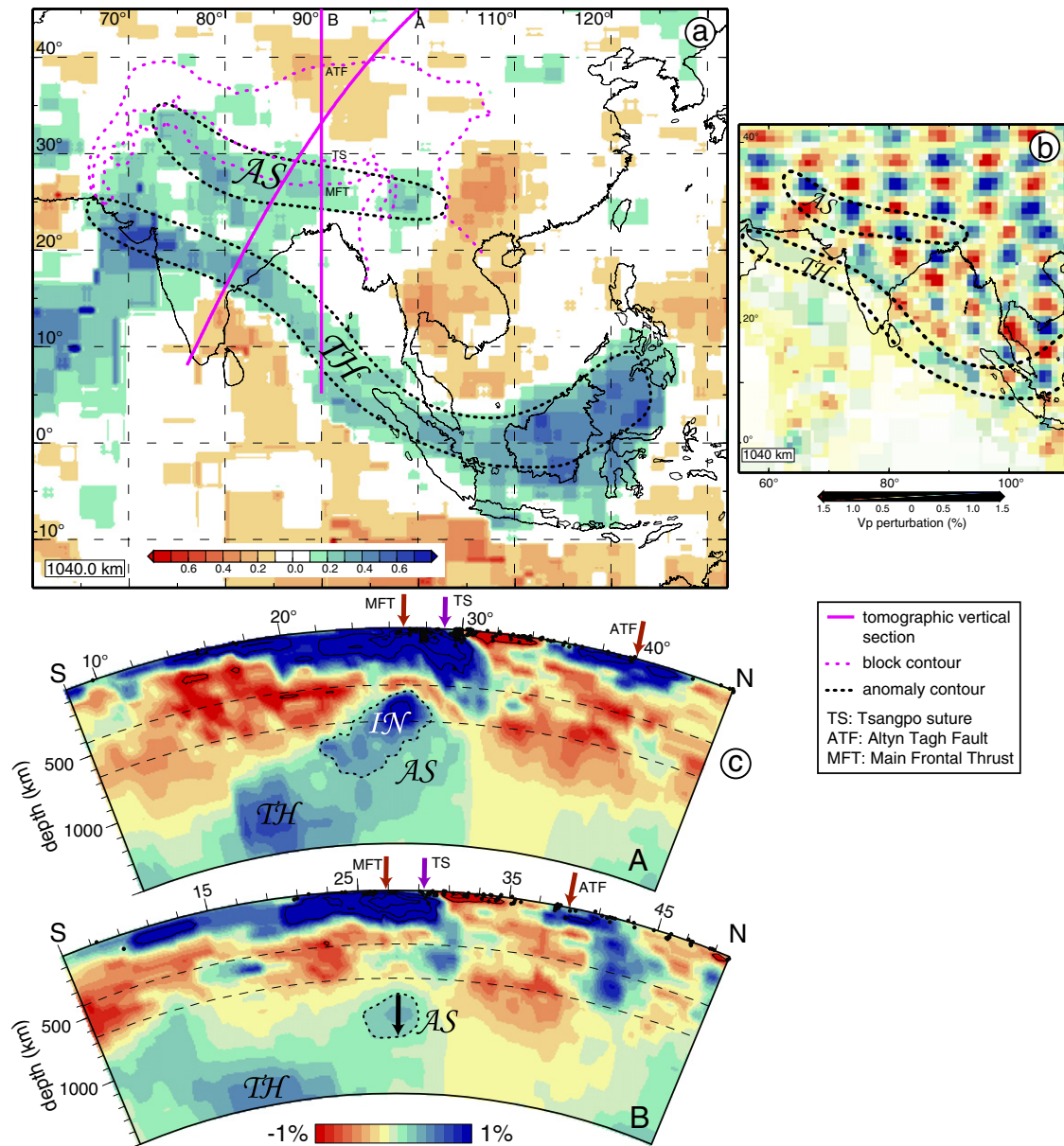
Fig. 2. a) Tomographic section at 1040 km depth showing two positive high-wavespeed anomalies TH and AS. The AS anomaly is located north of the TH anomaly and parallel to it for ~3000 km long. The elongated geometry of the AS anomaly and its position suggest that it is a remnant of slab related to a subduction event occurring north of the Tsangpo suture. b) Spike resolution tests for the Indian region at depths of 1040 km to obtain an estimate of the resolving power of the dataset. The input consist of 2° synthetic spikes with alternating ±5% velocity anomalies with respect to the reference model ak135 (Kennett et al., 1995). The mantle region between the spikes has a 0% anomaly value to allow detection of horizontal and vertical smearing effects between spikes. Synthetic data were generated from the global spike models by integration of the synthetic slowness along the same ray paths as used in the real data experiment. The result of the spike resolution tests is very good for all regions north of 20°N, and decreases in southern India, due to the lack of stations and earthquakes. The low amplitude AS anomaly (dotted black outline) is sufficiently well resolved by the travel time dataset used in this study. c) In cross-section, the anomaly AS is observed between 1100 and 900 km depths (section B). The prominent anomaly IN could mask the AS anomaly (section A). AS is not continuous up to the surface, showing that it is related to a slab detached from the surface. We favor the hypothesis that once the slab detached from the continent it sunk continuously in the mantle, as no slab accumulation in the transition zone occurred in the region. Considering that the AS anomaly is located north and at shallower depth than the TH anomaly, we propose that this anomaly AS (ASian) is the remnant of an episode of Asian continental subduction, occurring soon after the indentation initiation, ended by a slab break-off.

Garcia-Castellanos and Villaseñor, 2011). Velocity perturbations are determined with respect to the 1D reference model ak135 (Kennett et al., 1995). The model is parameterized with cell sizes depending on ray density, typically between 0.5° and 2° in the upper mantle and between 1° and 3° in the lower mantle (Spakman and Bijwaard, 2001).

Resolution of global travel-time tomography models with a large number of model parameters like the one used here cannot be estimated quantitatively using the resolution matrix because the inversion is carried out using iterative methods (Amaru, 2007; Amaru et al., 2008). The most common method for estimating the resolving power of the dataset is to conduct synthetic reconstruction tests.

Synthetic data were generated from the global spike models by integration of the synthetic slowness along the same ray paths as used in the real data experiment. The synthetic (checkerboard) models used here consist of well separated spikes with alternating ±5% velocity anomalies with respect to the reference model ak135 (Kennett et al., 1995) shifted laterally and in depth. We have used spike amplitudes of ±5% because they lead to a signal to noise ratio of the synthetic delays that is similar to that of real data when 0.5 s Gaussian noise is added (Amaru, 2007; Schellart et al., 2009). The mantle region between the spikes has a 0% anomaly value to allow detection of horizontal and vertical smearing effects between spikes.

Fig. 2b shows the results of the synthetic reconstruction test for 2°×2° spikes at 1040 km depth. For our studied area, the synthetic reconstruction models show good resolution beneath the continent, which decreases beneath the Indian Ocean, due to the lack of stations and earthquakes (Fig. 2). The anomaly AS (black dotted line, Fig. 2b) is located in a well resolved zone, with a good returned amplitude and reduced horizontal smearing. The TH anomaly is at the boundary of the well resolved zone for such spike size. The prominent TH anomaly is related to a wider anomaly than these 2°×2° spikes and appears in a well resolve zone with 3°×3° spike resolution tests (Replumaz et al., 2010b).

2.2. Deep anomaly AS

Between 1100 and 900 km depths, north of and parallel to the TH anomaly, a positive high-wavespeed anomaly of lower amplitude has been identified (labeled AS in Fig. 2; Hafkenscheid et al., 2006; Replumaz et al., 2010c). Our resolution test shows that the high-velocity-anomaly bodies AS and TH are separated, but not two parts of a large-scale tomographic feature. The size and location of the anomaly AS are well resolved by our travel-time dataset (Fig. 2b). The horizontal extent of the AS anomaly is ~3000 km. AS appears also separated from IN in depth, as AS is observed between 1100 and 900 km depths, under IN observed between 900 and 450 km depths (section A, Fig. 2). AS appears also separated from IN in latitude, as AS is observed north of IN, except at longitudes close to 80°E (see Replumaz et al., 2010b for precise cartography of the IN anomaly, and final figure of this paper), where the weak positive anomaly AS is masked by the prominent anomaly IN close to these longitudes (section A, Fig. 2). In contrast anomaly AS is more clearly observed in cross-sections where the anomaly IN is not present (section B, Fig. 2). Another indication for anomalies AS and IN being different features is the large difference in lateral extent, about 1500 km for IN and 3000 km for AS.

The geometry of the AS anomaly elongated and parallel to the anomaly TH (related to the Tethys subduction) suggests that it is also the signature of a remnant of slab (Fig. 2). We will argue in a later section that this anomaly AS (for ASian) is the remnant of an episode of Asian continental subduction post-dating and to the north of the Indian subduction episode related to the TH anomaly.

2.3. Positive high amplitude anomalies

The amplitude of mapped positive anomalies is higher in the upper mantle than in the lower mantle (Fig. 2). We are aware that the anomaly amplitudes should be interpreted with caution as they are affected by many factors as the deep structure of the Earth, the algorithm of the inversion, the seismic data coverage (e.g. Bijwaard et al., 1998; Amaru, 2007). Instead of interpreting specific values of amplitude, we only describe the first order systematic differences in amplitude between the positive anomalies observed between the Indian and the Asian cratons. To the west, the round positive anomaly beneath India (+2–3%, Fig. 3) marks the thick and cold lithospheric mantle of the Indian craton (labeled CR, for Indian CRaton in Fig. 3), while weaker rounded positive anomalies (+1–2%) mark the other Asian cratons (Ordos, Sichuan and Tarim). Beneath the Tibetan Plateau, the mantle is quite heterogeneous (e.g. Li et al., 2008; Feng et al., 2011). To the south and to the west, a strong positive anomaly (2–3%) is continuous with the CR anomaly. To the east and to the north, a positive but weaker (1–2%) anomaly is related to the North China craton. Beneath the center of the Plateau, a negative anomaly is observed (Fig. 3). This anomaly could be related either to hotter temperature likely produced by lithospheric thinning (Jimenez-Munt et al., 2008), or to the presence of hydrated minerals, as hydrous minerals strongly reduce the viscosity of the lithosphere (Billen and Gurnis, 2001).

In cross-section the strong positive anomaly CR in the upper mantle beneath India is thick (~200 km, section D, Fig. 3b), while the weaker positive anomaly beneath Northern China is thinner (~100 km). The amplitude of the anomaly IN is similar to the amplitude and width of the anomaly CR (2–3%).

2.4. Mantle structure under the Tibetan Plateau

Closely spaced tomographic cross-sections show positive anomalies with very different geometries beneath the Tibetan Plateau (for serial sections see Li et al., 2008).

On the north–south section beneath central Tibet (section C, Fig. 4), the thick positive anomaly CR bends south of the Tsangpo suture and continues horizontally north of the Bangong suture. North of the bend, the anomaly CR is overlaid by a negative anomaly above 70 km depth. Beneath central Tibet, the anomaly is negative down to the lower mantle.

On the SW–NE section parallel to the Altyn Tagh Fault (section D, Fig. 4), the anomaly CR plunges south of the Bangong suture down to at least 400 km depth, as also observed by Li et al. (2008). Beneath Central Tibet, a negative anomaly is observed, as along section C. A positive anomaly TI plunges southwards down to about 200 km (section D, Fig. 4).

The plunging of the anomaly CR imaged in section D is not observed along the nearby cross-section E (Fig. 4). Instead, the anomaly CR bends and continues horizontally to 33°N. A continuous shallow positive anomaly is observed in this section beneath Tibet, and no clear south dipping positive anomaly can be identified.

3. Interpretation of seismic velocity anomalies

As mentioned before, we use the terms "continental subduction" to refer to the process of subduction of lower crust and underlying lithospheric mantle. For the Indian continent the upper crust scraps off forming the high Himalayan range, while the lower crust bends and is eclogitized (Hetenyi et al., 2007; Nábělek et al., 2009), and can easily subduct attached to the lithospheric mantle (Capitanio et al., 2010). We refer to these subducted portions of continental lithosphere as "continental slabs". In this section we interpret the positive anomaly AS and TI as Asian continental slabs.

3.1. Shallow tomographic anomaly CR and TI compared with seismic profiles

We compare our global tomographic cross-sections with published seismic profiles across the Himalayan range and the Tibetan Plateau obtained using the receiver function method (e.g. Kind et al., 2002; Tilmann et al., 2003; Nábělek et al., 2009). This method enhances converted S waves from P waves of distant earthquakes impinging on interfaces beneath the recording stations. We plot the major interfaces observed on the seismic profiles on the tomographic sections across Tibet (light green lines in Fig. 4).

Along the Hi-Climb seismic profile at ~90°E of latitude (Nábělek et al., 2009), the Indian Moho bends south of the Tsangpo suture and continues horizontally (section C, Fig. 4). The Moho is duplicated from the Tsangpo suture to 31°N latitude, with an upper interface at ~60 km depth and a second interface at 75 km depth. The double Moho has been related to the top and bottom of the Indian lower crust which eclogitized during bending (Hetenyi et al., 2007). Nábělek et al. (2009) interpreted the Indian Plate to stop at 31°N, where the double Moho stops and suggested a single interface lying between 60 and 70 km depths to the north of 31°N to be related to the Tibetan Moho (dotted green line, Fig. 4). The positive anomaly related to the Indian Craton (CR) bends consistently with this seismic profile (Fig. 4). North of the bending region, the anomaly CR suggests that the Indian craton continues horizontally north of the Bangong
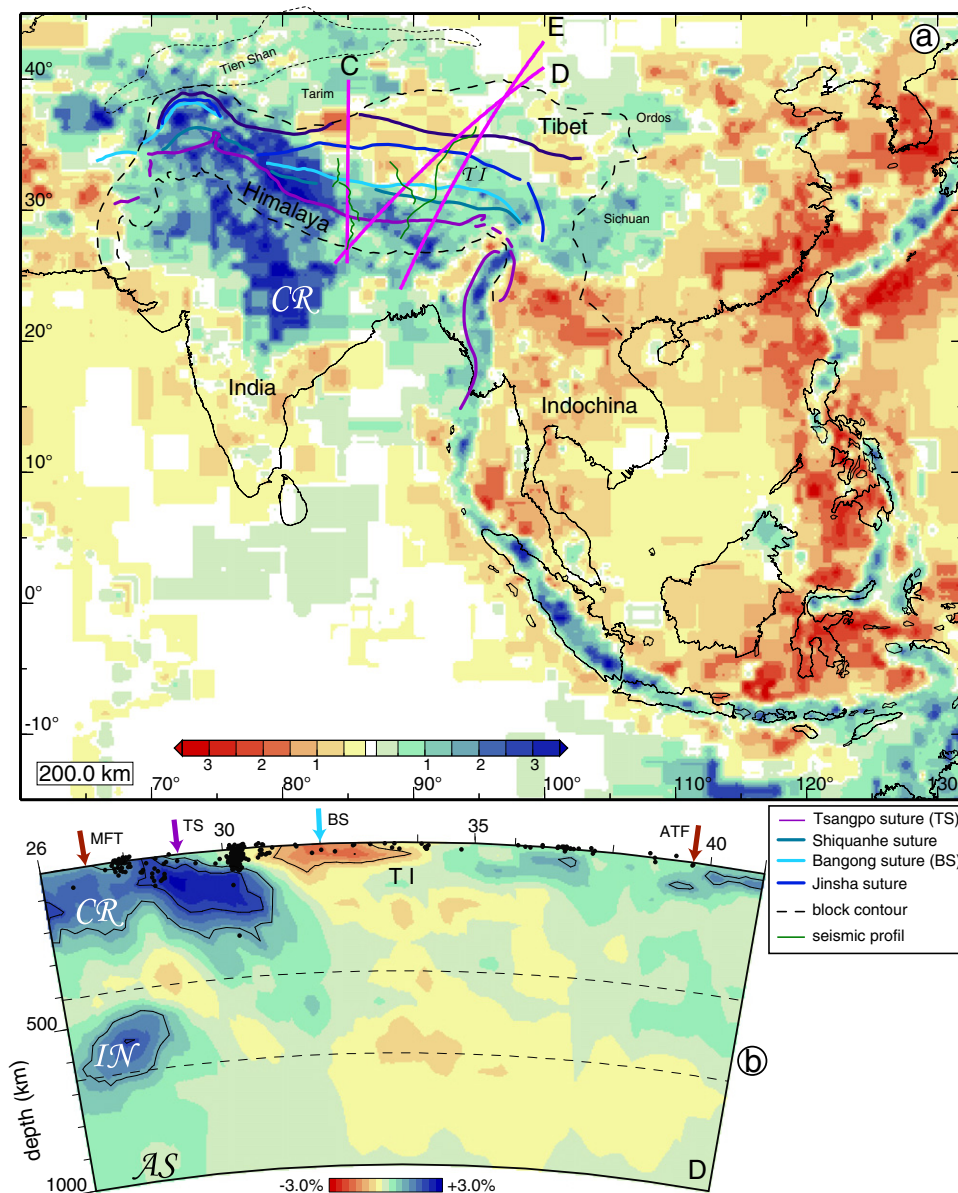
Fig. 3. a) Tomographic section at 200 km depth, showing wavespeed anomaly at −/+ 3%. Strong positive anomalies (+ 2–3%, blue) mark the cold Indian oceanic plate subducting beneath Indonesia and the cold lithospheric mantle beneath the Indian craton. Weaker positive anomalies (+ 1–2%) mark the other asian cratons (Ordos, Sichuan and Tarim), and the thickening of the Tien Shan. b) We use the same color bar in cross-section to emphasize the anomaly amplitude difference at depth. The strong positive anomaly beneath India is thick (~200 km), while the weaker positive anomaly beneath Northern China is thinner (~100 km, section E). The strong IN anomaly is related to the subduction of the Indian lithosphere (Replumaz et al., 2010). The weak anomaly TI is related to a present-day subduction event of the Asian lithosphere (Kind et al., 2002). We argue in this paper that the weak anomaly AS is related to an ancient subduction event of the Asian lithosphere. (For interpretation of the references to color in this figure legend, the reader is referred to the web version of this article.)

suture to 34°N (Fig. 4), farther north than interpreted from the Hi-Climb seismic profile, and is overlaid by the negative anomaly above 70 km depth, which is likely related to the Tibetan crust.

A compilation of several seismic experiments in Central Tibet reveals the existence of a south dipping interface extending to about 300 km (green line in section D, Fig. 4) that was interpreted as Asian lithospheric mantle (ALM; Kind et al., 2002). The plunging TI positive anomaly shown on the NW–SE section D is consistent with the ALM interface, except that the TI anomaly is observed only down to 200 km (Fig. 4). Along the Western Indepth profile two facing slabs have been interpreted (Tilmann et al., 2003), but due to the different trends between our section D and the Western Indepth profile, we could not precisely compare the geometry of the anomalies between both sections, although the overall geometry is similar (see also Li et al., 2008).

3.2. Deep anomaly AS related to Asian continental slab

The geometry of the AS anomaly, elongated and parallel to the suture zones crossing the Tibetan Plateau (Fig. 2), suggests that it is the signature of a remnant of slab. The anomaly vanishes at depths shallower than about 900 km, thus indicating that the slab was detached from the surface by a slab break-off process. Once the slab was detached from the continent, it may have sunk continuously through the transition zone or may have stagnated for a while in the upper mantle, as proposed by Hafkenscheid et al. (2006). Although stagnation cannot be ruled out, we consider that continuous sinking with a reduced velocity in the lower mantle is more likely to occur in this area. Steep subduction associated with fixed or advancing trenches is more favorable for direct penetration of slabs into the lower mantle (Manea and Gurnis, 2007) except for models where an
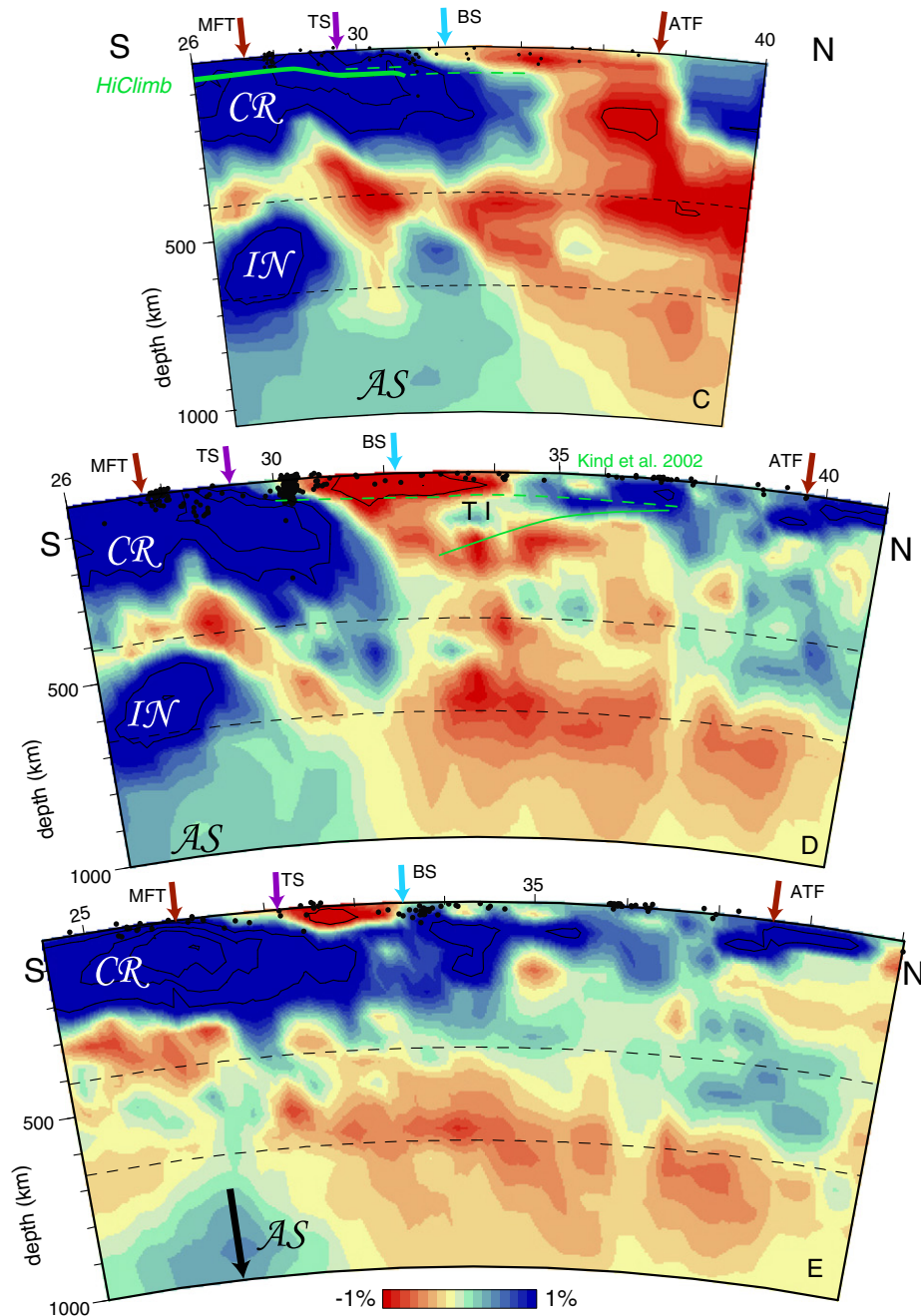
Fig. 4. Three tomographic sections across Tibet (see Fig. 2 for location) showing high structural variability across the Tibetan Plateau. Section C: the positive anomaly CR (Indian Craton) bends and continues horizontally north of the Bangong suture (BS). Thick green line shows the bending of the Indian craton imaged by the Hi-Climb profile (Nábělek et al., 2009). Section D: the positive anomaly CR bends north of the Indus–Tsangpo suture and plunges down to at least 400 km depth. The positive anomaly TI plunges to the south compatible with the plunging of Northern Tibet lithosphere observed by Kind et al., 2002 (green line). Section E: the anomaly CR bends and continues horizontally. The northern limit of CR is unclear as the negative anomaly beneath central Tibet is not observed along this section. (For interpretation of the references to color in this figure legend, the reader is referred to the web version of this article.)

impermeable barrier is imposed at the base of the upper mantle (e.g. Capitanio et al., 2010). Actually, the portion of detached continental slab represented by the prominent anomaly IN indicates direct penetration into the lower mantle. Another clear example in the area of continuous sinking across the transition zone without any slab stagnation is the subduction zone surrounding Southeast Asia. Considering continuous sinking, the position of the AS anomaly at shallower depth than anomaly TH suggests that the anomaly AS is the signature of an episode of subduction occurring after the break-off process that detached the Tethys oceanic root. This episode of subduction therefore likely occurred at the beginning of the indentation of Asia by India.

We also consider that no significant horizontal motion of subducted lithosphere occurs in the area, as previously inferred from the coincidence between the location of subducted slabs and the location of the reconstructed plate boundary at the time of subduction (e.g. Replumaz et al., 2004). In the absence of slab stagnation and horizontal motion, we consider that the AS anomaly is too far north and too shallow to represent a fragment of Tethyan slab subducted before collision. Instead, we propose that this anomaly AS (Asian) is the signature of an episode of Asian continental subduction. This continental subduction process ended by a slab break-off allowing the slab to sink into the mantle.

3.3. Including successive episodes of Asian subduction in tectonic scenario

We integrate the Asian subduction events related to anomalies AS and TI with published tectonic reconstructions of Replumaz and Tapponnier (2003) to relate the subduction events to the surface evolution of the region (Fig. 5).

A sequence of Indian subduction events during collision has been proposed by Replumaz et al. (2010a) and is briefly summarized here. The break-off of the oceanic root (anomaly TH) of the Indian continent at 45 Ma (Negredo et al., 2007) was followed by Indian impingement upon the Asian margin. A second episode of Indian subduction related to the anomaly IN most probably occurred between 40 and 15 Ma (Replumaz et al., 2010b). A narrow slice of Indian lithosphere remaining to the west subducted since about 8 Ma beneath the Hindu Kush (Negredo et al., 2007). To the east, partial extrusion of the Indian lithosphere was contemporaneous with the Indochina extrusion (Replumaz et al., 2010a). In central Tibet, one narrow zone of steep Indian subduction is observed (Fig. 4, section D; Tilmann et al., 2003; Li et al., 2008).

We here complement this proposed sequence of events (Fig. 5). We postulate that the first episode of Asian subduction, indicated by the anomaly AS, occurred after the Indian oceanic-root slab break-off. The position of anomaly AS above TH and below IN, suggests this Asian subduction episode occurred between the two Indian subduction
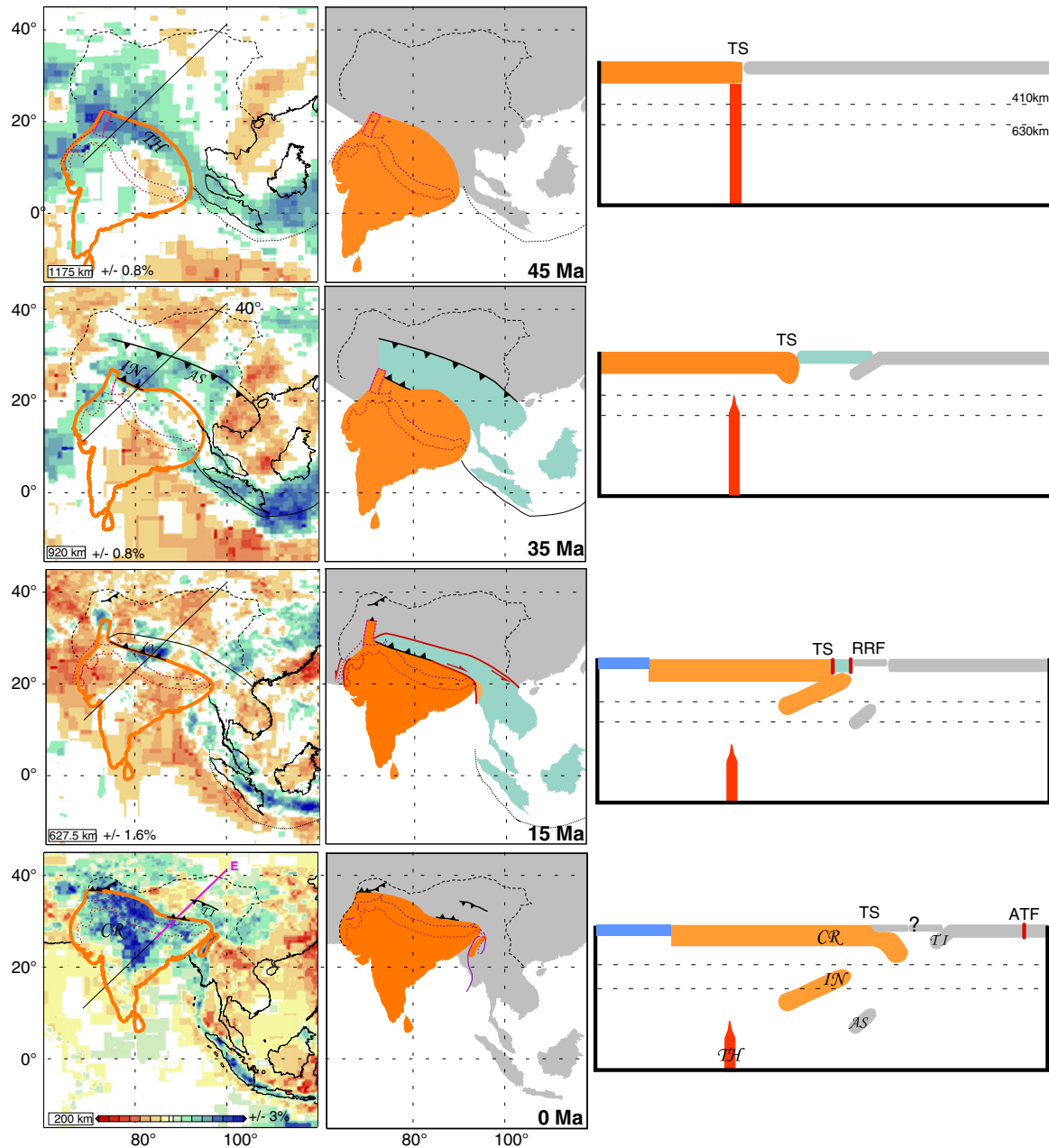
Fig. 5. We combine tomographic sections at different depths (left column) with tectonic reconstruction position at different times (Replumaz and Tapponnier, 2003) to constrain the timing and locations of different subduction events during the collision. We draw schematic maps (middle column) and cross-sections (right column) showing successive subduction events related to positive anomalies observed at depth (TH, AS, IN, TI).1175 km: top of anomaly TH related to the break-off of the Tethys oceanic root of the Indian continent at ~45 Ma.920 km: anomaly AS related to a southward subduction of Asian subduction facing the anomaly IN related to the northward Indian subduction occurring between 40 and 15 Ma (Replumaz et al., 2010).627 km: top of anomaly IN, related to the break-off of Indian slab at ~15 Ma.200 km: anomaly CR showing the extent of the Indian lithosphere and shallow anomaly TI related to the present-day southward Asian subduction (Kind et al., 2002). In cross-section, this stage represents the mantle structure as it is observed by global tomography, with the deep anomalies TH, IN and AS, and the shallow anomalies CR and TI.

episodes and may have concluded before the initiation of Indochina extrusion at 32 Ma (Leloup et al., 2001). In the western part of the collision zone, a narrow portion of Asian lithosphere began subducting beneath the Pamir at about 25 Ma (Burtman and Molnar, 1993). In central Tibet, ongoing south-directed Asian subduction is correlated to the anomaly TI (Fig. 4, section D), in agreement with the interpretation by Kind et al. (2002).

High lateral variability in mantle structure imaged in different cross-sections across the collision range suggests that, except for the subduction processes related to anomalies TH and AS, the lateral extent of subduction processes is limited (Fig. 4).

3.4. Magmatism related to successive Asian subduction episodes

Widespread Cenozoic magmatism throughout Tibet is interpreted as the result of mixing between lower crust-derived melts (dominantly adakitic magma) and lithospheric mantle-derived ultrapotassic mafic melts (e.g. Arnaud et al., 1992; Chung et al., 2009). The lithospheric origin of these magmas suggests that they may serve as indicators for different episodes of subduction. Palaeocene magmatism observed south of the Bangong suture (Fig. 3) has been interpreted to be related to the Tethys oceanic slab break-off (top of anomaly TH, Fig. 5; Guo et al., 2012), while Eocene magmatism may be related to the Indian continental slab break-off (top of anomaly IN, Fig. 5; Guo et al., 2012). North of the Bangong suture, widespread potassium-rich lavas and subordinate sodium-rich basalts (45 to 33 Ma) are consistent with a source derived from melting of enriched lithospheric mantle (Roger et al., 2000; Ding et al., 2007). We suggest that this magmatism probably reflects the southward subduction of the northern Tibet related to anomaly AS.

4. Discussion: amount of Asian convergence and subduction during collision

To quantify the amount of convergence that is absorbed by Asian continental subduction since 45 Ma, we estimate the amount of convergence absorbed by Asia and the length of the Asian lithospheric slabs subducted since then. The total amount estimated for the convergence between India and Asia is ~2200 km, which corresponds to the distance between the present-day position of the Himalayan front and its paleo-position at 45 Ma deduced from the position of the TH anomaly (black arrow on Fig. 1a; Negredo et al., 2007). By comparing the southern paleo-boundary of the Asian continent drawn along the top of the TH anomaly and its present-day shape, we estimated that ~1300 km of convergence has been absorbed by Asia (pink arrow on Fig. 1b). The rest of the convergence, ~900 km, is then assumed to be absorbed by India, within the Himalayan range (blue arrow on Fig. 1b).

4.1. Length of slab related to anomaly AS

The amplitude of the anomaly AS is low (maximum + 0.5%, Fig. 2). It is related to a slab comparable with the North China craton lithosphere of + 1.5% maximum anomaly amplitude (north of ATF in Fig. 3) which has sunk into the lower mantle. Anomaly smearing and the partial loss of visibility of slabs as they penetrate into the lower mantle are common features of deep subduction zones (e.g. van der Hilst et al., 1997; Bijwaard et al., 1998; Ricard et al., 2005). For example, the subduction of the Indian lithosphere is related to anomalies whose maximum amplitude decreases with depth: the anomaly CR in the upper mantle is + 3%, the anomaly IN in the transition zone is 2% but in the lower mantle it reduces to 0.5% (Fig. 2). Due to the difficulty in estimating qualitatively the resolution of global travel-time tomography models like the one used here (see Section 2.1), it is difficult to calculate an uncertainty for the size of the slab related to the tomographic anomaly. We use the minimum velocity anomaly amplitude

which draws a block-like slab to estimate the length of a slab related to one anomaly. Replumaz et al. (2010b) used the contour 0.4% for the anomaly IN to estimate the slab length to 700 km (black dotted line section A, Fig. 2). The same decrease of amplitude with depth is observed between the maximum amplitude of the north China craton anomaly (1.5%), and the anomaly AS (0.4%). The contour at 0.2% velocity anomaly draws a block-like slab with a length of 200 km (black dotted line and arrow section B, Fig. 2).

Slab penetration into the lower mantle could lead to thickening or buckling of weak slabs (e.g. Christensen, 1996; Ribe et al., 2007). We estimate the thickening of the slab in the lower mantle using the sinking rate deduced locally by Replumaz et al. (2004) from the matching between age constraints of surface events and change in slab structure at a specific depth. The 700 km of extrusion of Indochina and 550 km of seafloor spreading in the South China Sea that reorganized southeast Asia between 40 and 15 Ma (Tapponnier et al., 1986; Replumaz and Tapponnier, 2003), is reflected by the large shifts in slab geometry between 1100 and 700 km depths. Replumaz et al. (2004) deduced that in this region sinking of cold lithosphere, apparently with little lateral advection in a mantle reference frame, took place at a rate of 2 cm/yr and 4 cm/yr in the lower and upper mantle, respectively (as also inferred by Grand et al., 1997; van der Hilst et al., 1997; van der Voo et al., 1999). With a sinking rate in the upper mantle similar to the Indian plate velocity since 50 Ma, little or no slab thickening is expected to occur. As the assumed sinking velocity decrease between the upper and the lower mantle is about 50%, the maximum shortening of the slab should be of the same order if a weak highly deformable slab is assumed. Considering a length of the anomaly AS of 200 km, the maximum initial length of the subducted Asian lithospheric mantle should be about 400 km. It represents the maximum amount of lithospheric mantle that could have been absorbed during the episode of continental subduction represented by anomaly AS.

4.2. Budget of lithospheric mantle absorbed during collision

Considering the maximum length of the Asian slab related to anomaly AS to be about 400 km and adding 200 km of the present-day length of Asian slab beneath central Tibet related to anomaly TI, we obtain a maximum amount of 600 km of Asian lithospheric mantle absorbed during continental subduction processes. Considering convergence absorbed by Asia during the indentation process to be ~1300 km (Fig. 1), it corresponds to a maximum of 45% of Asian lithospheric mantle absorbed by continental subduction.

Several hypotheses could be invoked to explain the accommodation of the rest of the Asian convergence. According to tectonic reconstructions, 30% of the convergence is likely accommodated by extrusion (Replumaz and Tapponnier, 2003; Replumaz et al., 2010a), corresponding to about 400 km. Other Asian slabs have been interpreted on the basis of seismic profiles, but are not taken into account in our estimations as they are not visible on our tomographic cross-sections. Meissner et al. (2004) imaged a north dipping slab rooted under the Bangong suture, which could correspond to a northward subduction of the South Tibet. The slab could be around 100 km long. Beneath the Bangong suture, Shi et al. (2004) interpreted a southward subduction of North Tibet down to 180 km. Moreover, low-velocity anomalies as observed beneath Central Tibet (Fig. 4), could be related to subduction of hydrated lithosphere, not visible in the tomographic model. Furthermore, Asian subduction processes could have been associated with underthrusting beneath Asian lithosphere, which could have locally doubled the Asian lithosphere (Nábĕlek et al., 2009; Feng et al., 2011).

5. Conclusions

Using global seismic tomography images, we interpret the existence of successive Asian continental subduction events. A lower mantle positive anomaly (AS) is interpreted as the remnant of an

Asian subduction process occurring soon after the 45 Ma break-off that caused the detachment of the previously subducted oceanic slab from continental India. The anomaly AS is observed between 1100 and 900 km depths, along 3000 km parallel to the Southern Asian margin and probably represents the initial south dipping subduction of North Tibet zone occurring by Eocene to Oligocene time. Two narrow Asian presently subducting slabs, one to the west beneath Pamir and one to the east of Central Tibet are observed.

After 45 Ma, we estimate that the convergence absorbed by Asia during the indentation process is ~1300 km, with a maximum amount of about 600 km of Asian lithospheric mantle absorbed by continental subduction during the collision. It corresponds to a maximum of 45% of the Asian convergence. The rest could have been accommodated by a combination of extrusion and shallow subduction/underthrusting processes.

We conclude that continental subduction of the Asian plate plays a major role in absorbing the convergence during collision with India, and is therefore a major lithospheric process involved in intraplate tectonics of a supercontinent like Eurasia.

Acknowledgments

References

Amaru, M., 2007. Global travel time tomography with 3-D reference models. PhD thesis, Utrecht University, Utrecht.

Amaru, M.L., Spakman, W., Villaseñor, A., Sandoval, S., Kissling, E., 2008. A new absolute arrival time data set for Europe. Geophysical Journal International 173, 465–472. http://dx.doi.org/10.1111/j.1365-246X.2008.03704.x.

Arnaud, N.O., Vidal, P., Tapponnier, P., Matte, P., Deng, W., 1992. The high K₂O volcanism of northwestern Tibet: geochemistry and tectonic implication. Earth and Planetary Science Letters 111, 351–367.

Besse, J., Courtillot, V., 2002. Apparent and true polar wander and the geometry of the geomagnetic field over the last 200 Myr. Journal of Geophysical Research 107. http://dx.doi.org/10.1029/2000JB000050.

Bijwaard, H., Spakman, W., Engdahl, E.R., 1998. Closing the gap between regional and global travel time tomography. Journal of Geophysical Research 103, 30055–30078.

Billen, M.I., Gurnis, M., 2001. A low viscosity wedge in subduction zones. Earth and Planetary Science Letters 193, 227–236. http://dx.doi.org/10.1016/S0012-821X(01)00482-4.

Burtman, V.S., Molnar, P., 1993. Geological and geophysical evidence for deep subduction of continental crust beneath the Pamir. Special Paper-Geological Society of America 281, 76.

Capitanio, F.A., Morra, G., Goes, S., Weinberg, R.F., Moresi, L., 2010. India–Asia convergence driven by the subduction of the Greater Indian continent. Nature Geoscience 3, 136–139. http://dx.doi.org/10.1038/NGEO725.

Chemenda, A.I., Burg, J.P., Mattauer, M., 2000. Evolutionary model of the Himalaya–Tibet system: geopoem based on new modelling, geological and geophysical data. Earth and Planetary Science Letters 174, 397–409.

Christensen, U.R., 1996. The influence of trench migration on slab penetration into the lower mantle. Earth and Planetary Science Letters 140, 27–39.

Chung, S.L., Chu, M.F., Jinaqing, L., 2009. The nature and timing of crustal thickening in Southern Tibet: geochemical and zircon Hf isotopic constraints from post-collisional adakites. Tectonophyics 477, 36–48.

De Celles, P.G., Robinson, D.M., Zandt, G., 2002. Implications of shortening in the Himalayan fold–thrust belt for uplift of the Tibetan Plateau. Tectonics 21. http://dx.doi.org/10.1029/2001tc001322.

de Sigoyer, J., Chavagnac, V., Blichert-Toft, J., Villa, I.M., Luais, B., Guillot, S., Cosca, M., Mascle, G., 2000. Dating the Indian continental subduction and collisional thickening in the northwest Himalaya: multichronology of the Tso Morari eclogites. Geology 28, 487–490.

Ding, L., Kapp, P., Yue, Y., Lai, Q., 2007. Postcollisional calc-alkaline lavas and xenoliths from the southern Qiangtang terrane, central Tibet. Earth and Planet Science Letters 254, 28–38.

Engdahl, E.R., van der Hilst, R.D., Buland, R.P., 1998. Global teleseismic earthquake relocation with improved travel times and procedures for depth determination. Bulletin of the Seismological Society of America 88, 722–743.

England, P.C., Houseman, G.A., 1988. The mechanics of the Tibetan plateau. Philosophical Transactions of the Royal Society of London A326, 301–320.

Feng, M., An, M., Xue, G., Mechie, J., Zhao, Y., 2011. Lithosphere structures of northeast Tibetan Plateau and their geodynamic implications. Journal of Geodynamics 52, 432–442.

Garcia-Castellanos, D., Villaseñor, A., 2011. Messinian salinity crisis regulated by competing tectonics and erosion at the Gibraltar arc. Nature 480. http://dx.doi.org/10.1038/nature10651.

Garzanti, E., Baud, A., Mascle, G., 1987. Sedimentary record of the northward flight of India and its collision with Eurasia (Ladakh Himalaya, India). Geodinamica Acta 1, 297–312.

Garzanti, E., Critelli, S., Ingersoll, R.V., 1996. Paleogeographic and paleotectonic evolution of the Himalayan Range as reflected by detrital modes of tertiary sandstones and modern sands (Indus transect, India and Pakistan). Geological Society of America Bulletin 108, 631–642. http://dx.doi.org/10.1130/0016-7606(1996) 108<0631:PAPEOT>2.3.CO;2.

Grand, S.P., Van Der Hilst, R.D., Widiyantoro, S., 1997. Global seismic tomography; a snapshot of convection in the Earth. GSA Today 1–7.

Guillot, S., Garzanti, E., Baratoux, D., Marquer, D., Maheo, G., de Sigoyer, J., 2003. Reconstructing the total shortening history of the NW Himalaya. Geochemistry, Geophysics, Geosystems 4. http://dx.doi.org/10.1029/2002gc000484.

Guillot, S., Mahéo, G., de Sigoyer, J., Hattori, K.H., Pêcher, A., 2008. Tethyan and Indian subduction viewed from the Himalayan high- to ultrahigh-pressure metamorphic rocks. Tectonophyics. http://dx.doi.org/10.1016/j.tecto.2007.11.059.

Guo, L., Zhang, H.F., Harris, B.W., Parrish, R., Xu, W.C., Shi, Z.L., 2012. Paleogene crustal anatexis and metamorphism in Lhasa terrane, eastern Himalayan syntaxis: evidence from U–Pb zircon ages and Hf isotopic compositions of the Nyinchi complex. Gondwana Research 21, 100–111.

Hafkenscheid, E., Wortel, M.J.R., Spakman, W., 2006. Subduction history of the Tethyan region derived from seismic tomography and tectonic reconstructions. Journal of Geophysical Research 111. http://dx.doi.org/10.1029/2005jb003791.

Halim, N., Cogne, J.P., Chen, Y., Atasiei, R., Besse, J., Courtillot, V., Gilder, S., Marcoux, J., Zhao, R.L., 1998. New cretaceous and early tertiary paleomagnetic results from Xining–Lanzhou Basin, Kunlun and Qiangtang blocks, China: implications on the geodynamic evolution of Asia. Journal of Geophysical Research 103 (21), 21,025–21,045.

Hetenyi, G., Cattin, R., Brunet, F., Bollinger, L., Vergne, J., Nabelek, J., Diament, M., 2007. Density distribution of the India plate beneath the Tibetan plateau: geophysical and petrological constraints on the kinetics of lower-crustal eclogitization. Earth and Planetary Science Letters 264. http://dx.doi.org/10.1016/j.epst.2007.09.036.

Jimenez-Munt, I., Fernandez, M., Verges, J., Platt, J.P., 2008. Lithosphere structure underneath the Tibetan Plateau inferred from elevation, gravity and geoid anomalies. Earth and Planetary Science Letters 267, 276–289. http://dx.doi.org/10.1016/s0012-821x(04)0070-6.

Kennett, B.L.N., Engdahl, E.R., Buland, R., 1995. Constraints on seismic velocities in the earth from travel-times. Geophysical Journal International 122, 108–124.

Kind, R., Yuan, X., Saul, J., Nelson, D., Sobolev, S.V., Mechie, J., Zhao, W., Kosarev, G., Ni, J., Achauer, U., Jiang, M., 2002. Seismic images of crust and upper mantle beneath Tibet: evidence for Eurasian plate subduction. Science 298, 1219–1221.

Le Pichon, X., Fournier, M., Jolivet, L., 1992. Kinematics, topography, shortening, and extrusion in the India–Eurasia collision. Tectonics 11, 1085–1098.

Leech, M.L., Singh, S., Jain, A.K., Klemperer, S.L., Manickavasagam, R.M., 2005. The onset of India–Asia continental collision: early, steep subduction required by the timing of UHP metamorphism in the western Himalaya. Earth and Planetary Science Letters 234, 83–97. http://dx.doi.org/10.1016/j.epsl.2005.02.038.

Leloup, P.H., Arnaud, N., Lacassin, R., Kienast, J.R., Harrison, T.M., Trong, T.T.P., Replumaz, A., Tapponnier, P., 2001. New constraints on the structure, thermochronology, and timing of the Ailao Shan-Red River shear zone, SE Asia. Journal of Geophysical Research 106, 6683–6732.

Li, C., van der Hilst, R.D., Meltzer, A.S., Engdahl, E.R., 2008. Subduction of the Indian lithosphere beneath the Tibetan Plateau and Burma. Earth and Planetary Science Letters 274. http://dx.doi.org/10.1016/j.epsl.2008.07.016.

Manea, V., Gurnis, M., 2007. Subduction zone evolution and low viscosity wedges and channels. Earth and Planetary Science Letters 264, 22–45. http://dx.doi.org/10.1016/j.epsl.2007.08.030.

Mattauer, M., 1986. Intracontinental subduction, crust–mantle décollement and crustal-stacking wedge in the Himalayas and other collision belts. Journal of Geological Society London Special Publications 19, 37–50.

Meissner, R., Tilmann, F., Haines, S., 2004. About the lithospheric structure of central Tibet, based on seismic data from the INDEPTH III profile. Tectonophyics 380, 1–25. http://dx.doi.org/10.1016/j.tecto.2003.11.007.

Molnar, P., Stock, J.M., 2009. Slowing of India's convergence with Eurasia since 20 Ma and its implications for Tibetan mantle dynamics. Tectonics 28, TC3001. http://dx.doi.org/10.1029/2008TC002271.

Nábělek, J., Hetényi, G., Vergne, J., Sapkota, S., Kafle, B., Jiang, Mei, Heping, Su., Chen, John, Huang, Bor-Shouh, the Hi-CLIMB Team, 2009. Underplating in the Himalaya–Tibet collision zone revealed by the Hi-CLIMB experiment. Science 325. http://dx.doi.org/10.1126/science.1167719.

Negredo, A.M., Replumaz, A., Villaseñor, A., Guillot, S., 2007. Modeling the evolution of continental subduction processes in the Pamir-Hindu Kush region. Earth and Planetary Science Letters 259. http://dx.doi.org/10.1016/j.epsl.2007.04.043.

Patriat, Ph., Achache, J., 1984. India–Eurasia collision chronology has implications for crustal shortening and driving mechanisms of plates. Nature 311, 615–621.

Replumaz, A., Tapponnier, P., 2003. Reconstruction of the deformed collision zone between India and Asia by backward motion of lithospheric blocks. Journal of Geophysical Research 108. http://dx.doi.org/10.1029/2001jb000661.

Replumaz, A., Karason, H., van der Hilst, R.D., Besse, J., Tapponnier, P., 2004. 4-D evolution of SE Asia's mantle from geological reconstructions and seismic tomography. Earth and Planetary Science Letters 221. http://dx.doi.org/10.1016/s0012-821x(04)00070-6.

Replumaz, A., Negredo, A.M., Guillot, S., Villaseñor, A., 2010a. Multiple episodes of continental subduction during India/Asia convergence: insight from seismic tomography and tectonic reconstruction. Tectonophysics. http://dx.doi.org/10.1016/j.tecto.2009.10.007.

Replumaz, A., Negredo, A.M., Guillot, S., van der Beek, P., Villaseñor, A., 2010c. Crustal mass budget and recycling during the India/Asia collision. Tectonophysics. http://dx.doi.org/10.1016/j.tecto.2009.10.007.

Replumaz, A., Negredo, A.M., Villaseñor, A., Guillot, S., 2010b. Indian continental subduction and slab break-off during Tertiary Collision. Terra Nova. http://dx.doi.org/10.1111/j.1365-3121.2010.00945.x.

Ribe, N.M., Stutzmann, E., Ren, Y., van der Hilst, R.D., 2007. Buckling instabilities of subducted lithosphere beneath the transition zone. Earth and Planetary Science Letters 254. http://dx.doi.org/10.1016/j.epsl.2006.11.028.

Ricard, Y., Mattern, E., Matas, J., 2005. Synthetic tomographic images of slabs from mineral physics. In: van der Hilst, R.D., Bass, J., Mattas, J., Trampert, J. (Eds.), Earth's Deep Mantle, Structure Composition, and Evolution, Vol. 160, Geophysical Monograph. AGU, Washington, pp. 283–300.

Richards, S., Lister, G., Kennett, B., 2007. A slab in depth: three-dimensional geometry and evolution of the Indo-Australian plate. Geochemistry, Geophysics, Geosystems 8. http://dx.doi.org/10.1029/2007gc001657.

Roger, F., Tapponnier, P., Arnaud, N., Scharer, U., Brunel, Xu, Z.Q., Yang, J.S., 2000. An Eocene magmatic belt across central Tibet: mantle subduction triggered by the Indian collision? Terra Nova 12, p102–p108. http://dx.doi.org/10.1046/j.1365-3121.2000.00282.x.

Schellart, W.P., Kennett, B.L.N., Spakman, W., Amaru, M., 2009. Plate reconstructions and tomography reveal a fossil lower mantle slab below the Tasman Sea. Earth and Planetary Science Letters 278. http://dx.doi.org/10.1016/j.epsl.2008.11.004.

Shi, D., Zhao, W., Brown, L.D., Nelson, D., Zhao, X.L., Kind, R., Xiong, J., Mechie, J., Guo, J., Klemperer, S.L., Hearn, T., 2004. Detection of southward intracontinental subduction of Tibetan lithosphere along the Bangong–Nujiang suture by P-to-S converted waves. Geology 32, 209–212.

Spakman, W., Bijwaard, H., 2001. Optimization of cell parameterizations for tomographic inverse problems. Pure and Applied Geophysics 158, 1401–1423.

Tapponnier, P., Peltzer, G., Armijo, R., 1986. On the mechanics of the collision between India and Asia. In: Ramsay, J.G., Coward, M.P., Ries, A.C. (Eds.), Collision Tectonics: Geological Society of London Special Publication, 19, pp. 115–157.

Tapponnier, P., Xu, Z.Q., Roger, F., Meyer, B., Arnaud, N., Wittlinger, G., Yang, J.S., 2001. Oblique stepwise rise and growth of the Tibet plateau. Science 294, 1671–1677.

Tilmann, F., Ni, J., Seismic Team, I.N.D.E.P.T.H.I.I.I., 2003. Seismic imaging of the downwelling Indian lithosphere beneath central Tibet. Science 300, 1424. http://dx.doi.org/10.1126/science.1082777.

van der Hilst, R.D., Widiyantoro, S., Engdahl, E.R., 1997. Evidence for deep mantle circulation from global tomography. Nature 386, 578–584.

van der Voo, R., Spakman, W., Bijwaard, H., 1999. Tethyan subducted slabs under India. Earth and Planetary Science Letters 171, 7–20.

Villaseñor, A., Spakman, W., Engdahl, E.R., 2003. Influence of regional travel times in global tomographic models. Geophysical Research Abstracts 5 (abstr. EAE03-A-08614).

Willett, S.D., Beaumont, C., 1994. Subduction of Asian lithospheric mantle beneath Tibet inferred from models of continental collision. Nature 369, 642–645.